(illegible)
NAG1-886
217250

SUMMARY REPORT

ON

AN INTEGRATED AERODYNAMIC/PROPULSION STUDY FOR GENERIC AERO-SPACE PLANES BASED ON WAVERIDER CONCEPTS

NASA Grant NAG-1-886

May - September 1988

M.L. Rasmussen and G. Emanuel
University of Oklahoma
School of Aerospace and Mechanical Engineering
865 ASP AVENUE Room 212
NORMAN, OKLAHOMA 73019
(405) 325-5011

(NASA-CR-183389) AN INTEGRATED AERODYNAMIC/PROPULSION STUDY FOR GENERIC AERO-SPACE PLANES BASED ON WAVERIDER CONCEPTS Summary Report, May - Sep. 1988 (Oklahoma Univ.) 24 p CSCL 01C G3/05

N89-24315

Unclas
0217250

CONTENTS

1. INTRODUCTION

The design of trans-atmospheric vehicles, or aero-space planes as they have come to be known, places excruciating demands on present-day technology. These vehicles embrace the various requirements for space-transportation systems, civil transports, and military aircraft. They are envisaged to take off from a runway, accelerate to orbital speed, and then to descend and land in a conventional manner. The Mach-number range would be from 0 to 25. The aero-space plane must provide sustained hypersonic flight in the altitude range from 80,000 to 150,000 feet. In addition to atmospheric maneuverability, it must also provide for efficient orbital changes.

Recent progress in the aerodynamic design of high-speed aircraft has recognized the need for the blending of wings, bodies, and propulsion units. The calculation of the flow fields and aerodynamics of such blended bodies is not accurately done by the semi-empirical merging of the calculations for the separate parts. Thus elaborate computer codes are used for the prediction of the flows involved. In many respects, these codes are still in the developmental stages and are expensive and unsuitable for many design studies. They are used to best advantage when guided by a simplified analysis that has first shown the direction for optimizing an aero-space plane.

The objective of this NASA grant is to provide a unified aero-space plane analysis based on waverider technology. The project is thus concerned with the overall aerodynamic design and performance of an aero-space plane. The vehicle is divided into three parts: a forebody, a scramjet, and an afterbody.

This is the first summary report in which we document the progress made during the first four months of the program. Sections 2-5 discuss specific topics, while a summary is provided in section 6. For the benefit of the reader, we briefly outline sections 2-5 and mention the status of each topic.

Section 2 discusses material covered in a full-length report entitled, "A First Scramjet Study," that was submitted to NASA Langley in August 1988. The effort devoted to this theoretical analysis is viewed as complete. The report consists of two parts. In the first, a general discussion of scramjets is provided that forms the basis for the parametric model of the second part. The model is a highly simplified one; it is utilized to provide insight into some of the dominant processes associated with a scramjet.

Section 3 is work in progress in which an alternate view of the scramjet is taken. For instance, the analysis described in section 2 does not account for shock waves and uses Mach number as the principal independent parameter. The section 3 analysis includes a shock wave and a heat addition distribution for a fixed geometry.

Section 4 briefly outlines a new approach for integrating a cone-based waverider forebody configuration with a scramjet and nozzle. This effort should be underway shortly. The ideas behind the concept are a natural outgrowth of the other efforts described in this report.

In section 5 we describe a comprehensive effort to analyze a two-dimensional, half exposed nozzle. A model has been fully formulated and its implementation is underway. The model has many features which enable it to provide thrust, lift, pitching moment, skin friction losses, and heat transfer, as well as other properties of the nozzle.

2. A FIRST SCRAMJET STUDY

This report documents a variety of related scramjet engine topics in which primary emphasis is on simplicity and conceptual clarity. Thus, the flow is assumed to be one dimensional and the gas is thermally and calorically perfect.

To lay the groundwork for the subsequent discussion, Sect. II in the report evaluates the thrust and lift of an exposed half nozzle and one that is fully confined. The section then concludes with a rough estimate of the drag of an aero-space plane. This estimate is needed to calibrate the thrust estimates provided in Sect. IV. Section III also presents background material, which is useful in the following sections. Thermal considerations and shock waves are the principal topics discussed.

A parametric scramjet model, based on the influence coefficient method, is provided in Sect. IV. Although elementary, the model evaluates some of the dominant scramjet processes to first order. The model assumes isentropic flow upstream of the combustor, a variable cross-sectional area heat addition process for the combustor, and an isentropic process for the external nozzle. A number of constraints are imposed for purposes of making the model more realistic. For instance, an overly extreme area variation for the combustor is avoided, and a maximum static temperature limitation is imposed. In line with this approach, the free stream Mach number is limited to the modest range of five to nine.

A parametric study, based on the model, is provided in Sect. V of the report. We conclude that a sonic velocity combustor condition maximizes the thrust. When this condition is not obtainable, as is often the case, the lowest attainable supersonic Mach number for the combustor is then optimum. This statement implies a constant Mach number heat addition process. We prefer this process over a constant pressure one, which is associated with the

Brayton cycle, or a constant area process, which readily results in thermal choking. The constant Mach number process is always free of choking difficulties, results in an acceptable combustor area variation, and yields a favorable pressure gradient. The later property is highly desirable for inhibiting boundary-layer separation.

Any combustor whose cross-sectional area increases with distance will produce thrust. This is always the case with heat addition and a constant combustor Mach number. Thus, both the nozzle and combustor produce thrust, where the fraction of the overall thrust generated by the combustor is often appreciable. It may, in fact, exceed the nozzle's thrust. The large thrust of the combustor is due, in part, to the relatively high pressure inside it.

If various Mach numbers, the ratio of specific heats, γ, and a nondimensional heat addition parameter, Q, are fixed, then the thrust due to the combustor and the nozzle are individually determined. Our discussion here does not assume a constant Mach number or inviscid flow for the combustor. In this circumstance, the report shows that the total thrust is independent of the Mach number at the combustor's exit. Consequently, there is no point in maximizing the combustor's thrust, since the overall thrust remains fixed. We emphasize that this conclusion assumes fixed Mach numbers at the combustor's inlet and at the exit of the nozzle.

Along with γ, Q, and two other Mach numbers, the model presumes given values for the Mach numbers at the inlet and exit of an inviscid combustor. A constant Mach number combustor is thus not required by the model, and a variety of cases are presented where this assumption is not utilized. Even when the combustor's entrance and exit Mach numbers are the same, the Mach number may still vary with distance inside the combustor, since its distribution is controlled by the area variation and skin friction, as well as

the rate of heat addition. Within the context of the model, which is inviscid, the distribution with distance of the heat addition has no effect on the overall thrust once Q is prescribed. The conclusions of the model, therefore, are insensitive to this distribution.

We briefly mention some of the principle conclusions that stem from the parametric study in the report that have not already been discussed. The thrust increases with an increase in the free stream Mach number. Moreover, the magnitude of the thrust is sensitive to both this Mach number and the combustor inlet Mach number. The thrust is also sensitive to γ, increasing rapidly as γ decreases. This effect is due to the large compression that occurs in the forebody and in the scramjet inlet.

3. COMBUSTION/NOZZLE OPTIMIZATION

The analysis described in "A First Scramjet Study" is being used as a basis for further studies. In these studies, the one-dimensional equations of motion are integrated numerically for specified combustor/nozzle shapes, and friction is taken into account. Hydrogen fuel is assumed to undergo uniform and complete combustion over an arbitrarily specified section of a prescribed combustor/nozzle geometry. The section over which the combustion occurs is varied, and for each case, the Mach number, temperature, and pressure distributions are obtained. In addition, the thrust, produced by each combustor/nozzle configuration is obtained.

Figure 1 shows a typical converging-diverging nozzle configuration under study. The first third is the converging diffuser section. The coordinate x along the nozzle configuration starts at $x = 0$ at the throat. Thus, the diffuser exists in the initial region $-1/3 < x/L < 0$, and the diverging nozzle section exists in the remainder, $0 < x/L < 2/3$, where L is the overall length. The combustion region is to be studied by placing it in some portion of this configuration. In the results to be shown here, the converging-diverging nozzle corresponds to an area distribution such that the Mach number is 5 at the entrance, 3.5 at the throat, and 8 at the exit according to inviscid adiabatic flow with $\gamma = 1.4$. If the geometrical configurations were axisymmetric, then the radius distribution would be as shown in Fig. 1. Within the framework of the one-dimensional analysis, the area distribution is not restricted to being axisymmetric or even symmetrical.

The flow friction is approximated by an average skin friction coefficient, c_f, over the whole converging-diverging nozzle length. The effect of the average skin friction coefficient is shown in Fig. 2 for flows without combustion. Positive thrust occurs when the exit Mach number is greater than the inlet Mach number, in this case, $M_i = 5$. In the subsequent

calculations shown here, the value $c_f = 0.002$ was used.

Figure 3 shows the effect of combustion location on the Mach number distribution. The combustion occurs over one third of the length, but the start of the burn occurs at x/L = - 1/8, 0, and 1/3. For these curves, $\gamma = 1.4$ was held fixed for all regions. The thrust ratio,

$$\frac{T}{\dot{m}\, a_t} \quad ,$$

where $\dot{m}$ is the mass flow rate and a_t is the speed of sound based on the total (stagnation) temperature at the inlet, is also shown in Fig. 3. For these comparative cases, the most thrust is produced when the burn starts at x/L = -1/8, that is, in the converging section.

Figure 4 shows the ratio of temperature to the initial total (stagnation) temperature for three burns starting at x/L = 0, but having burn lengths of L_b/L = 1/6, 1/3, and 2/3. The shorter burn length produces the larger largest thrust.

The figures shown in this section are indicative of the results that can be obtained by this sort of analysis. The complete study is the subject of an M.S. thesis by Mr. Carlos Soares, who intends to graduate in May 1989. The results are meant to be imbedded in a complete tip-to-tail analysis of a waverider-type configuration.

4. IDEALIZED TIP-TO-TAIL WAVERIDER MODEL

The basic design of a tip-to-tail waverider model stems from the idealized cone-derived waverider. This concept has been utilized previously for the waverider forebody and for the inlet cowl. The natural extension of this concept to include the afterbody into a complete tip-to-tail configuration is by means of a plug-nozzle flow to model the afterbody. The entire flow field of the basic configuration is thus axisymmetric.

Figure 5 shows the basic idealized cone-derived waverider. The dihedral angle is denoted by ϕ_{ℓ}. Figure 6 shows an axisymmetric inlet and cowl incorporated into the basic idealized waverider forebody design. The wrap-around half-angle of the cowl is denoted by ϕ_c, but in these figures we suppose that $\phi_c = \phi_{\ell}$. The outer surface of the cowl is a streamsurface of the basic cone flow, and its location can be varied in the analysis from the cone surface itself out to the conical bow shock. The compressed flow entering the scramjet inlet is uniform in stagnation enthalpy and stagnation pressure since the cone flow is homentropic. The flow is also nearly uniform across the shock layer such that a quasi-one-dimensional flow approximation is warranted for the flow entering the inlet cowl. Figure 7 shows a cross section and planform view of the idealized waverider that includes the plug nozzle afterbody.

Inside the scramjet near the inlet, a series of oblique shocks alter the properties and direction of the internal flow. In the model, the upstream-most shock can originate at either the cowl lip or on a forebody ramp. In the latter case, the shock would impinge on the lip of the cowl. The number of shocks and their individual strengths are prescribed.

The combustor is downstream of the last of the inlet shocks. The flow in this region is quasi-one-dimensional. The flow can be assumed to be a constant-Mach-number type, from which the cross sectional area can be

calculated or the cross-sectional area can be varied arbitrarily by means of other assumptions. The rate of heat addition is prescribed and all the flow properties are then calculated.

The afterbody is an external, exposed nozzle occurring downstream of the scramjet. At the exit of the scramjet and entrance to the nozzle, the flow is supersonic and the velocity orientation may be arbitrary. The nozzle itself is a section of an axisymmetric plug nozzle, with a dihedral angle of ϕ_c. Since plug nozzles may be longer than desired, a truncation procedure is included in the analysis.

A plug nozzle, as is true of a minimum length nozzle, provides a transitional axisymmetric flow field that terminates on a conical characteristic surface where the Mach number has its exit design value. This surface begins at the exit of the scramjet cowl and terminates in the truncation plane at the wall of the plug nozzle. The downstream end of the cowl should be parallel to the freestream velocity. Consequently, the outer surface of the scramjet's exhaust jet is cylindrical in shape, approximately at the freestream pressure, and is downstream of the above characteristic surface.

The external flow past the scramjet cowl is matched better with the afterbody plug nozzle if longitudinal curvature is introduced in the cowl shape so that the flow expands to nearly the freestream pressure. The effect of adding this longitudinal curvature on the total configuration is shown in Fig. 8.

The appropriate location of the truncation plane is to be determined by tradeoff studies. Several factors enter into these studies, such as the improvement of volumetric efficiency with early truncation. However, the dominant tradeoff is expected to be the decrease in drag and the decrease in

thrust as the location of the truncation plane is moved in an upstream direction. Near the apex of the untruncated nozzle, the rate of decrease with truncation of drag should exceed the thrust decrease rate. At some upstream location for truncation, the rates will cross.

A simple skin friction formulation is to be used. Thus, the effect of skin friction on the external as well as the internal flow is evaluated.

The model will predict all the usual aerodynamic parameters, such as volumetric efficiency, a viscous as well as inviscid lift to drag ratio, and the thrust. Upon completion, it will enable us to perform various design studies. In particular, these would include optimizing the volumetric efficiency and lift subject to the constraint that the thrust exceed the drag.

The configuration based on the idealized cone-derived waverider is simple and allows the basic design parameters to be identified and studied. A final, realistic configuration can be derived from the idealized shape. Streamsurfaces in the flow field of the configuration shown in Fig. 8 are to be used to obtain a final configuration. This is to be done by choosing a parabolic surface parallel to the axis of symmetry of the original basic cone and using it as a new freestream surface instead of the ridge shape of the idealized cone-derived waverider. The cone-flow streamlines that originate where this parabolic surface intersects the basic-cone shock are traced in the flow direction to form a new compression surface. When these streamlines are traced through the scramjet duct and out through the basic plug-nozzle flow, which is indicated in Fig. 8, they will form a new, blended forebody and a new blended afterbody external nozzle surface. This final type of configuration is shown in Fig. 9. The resulting body is a blended and integrated configuration, but the flow field is still axisymmetric, being part of a conical flow field and that of a plug nozzle.

5. TWO-DIMENSIONAL MINIMUM LENGTH NOZZLE INVESTIGATION

The scramjet is located on the lower surface, after which the afterbody is curved so as to provide an isentropic expansion of the exhaust gas. This part is called an exposed half nozzle, which is our primary interest. A high pressure and temperature gas, compressed by the forebody itself and its bow shock wave, enters into the scramjet. The gas temperature becomes even higher with the addition of fuel, and leaves the combustor at a supersonic speed. It then expands along the exposed nozzle that is the afterbody's undersurface. Some expansion occurs inside the combustor as well as along the nozzle, and both expansions generate thrust. An exposed half nozzle has several important advantages: the pressure along its upper surface, which is initially higher than in the freestream, generates a lift; radiation of heat away from this surface reduces the heat transfer, where it is most severe. Also, this type of nozzle reduces the size and weight of the vehicle. In contrast to an axisymmetric rocket nozzle, a two-dimensional nozzle is sometimes appropriate for the aero-space plane, in order to accommodate the flow field produced by the forebody's compression and take advantage of the lift that is generated by the pressure on the nozzle's upper wall.

The geometric shape of the exposed half nozzle closely resembles the upper half of a MLN, where the flow at the inlet surface is a source flow and the exit flow is a uniform flow. The shape of the upper wall can be based on the theory for a two-dimensional MLN with a cylindrical inlet surface. The inviscid theory for this flow is entirely analytical; a computer is used to reduce the computational effort for parametric studies.

In this investigation, the inlet surface may be sonic or supersonic with a Mach number M_i. For an exposed half nozzle, M_i usually exceeds unity because the combustion in the scramjet terminates at a supersonic speed. When $M_i > 1$, there is no sharp corner, as occurs with a sonic inlet surface, and

the rate of change of the cross-sectional area is not necessarily discontinuous. The formulation that is developed here, however, also covers the sonic inlet case for completeness. Hereafter, when we refer to the nozzle, it is understood that the Mach number at the inlet is equal to or greater than unity and that the nozzle is two-dimensional.

In addition to a geometrical analysis, a laminar boundary-layer analysis is provided to evaluate the skin friction, heat transfer, various viscous and thermal boundary-layer thicknesses, and accurate values of the thrust, lift, and pitching moment generated by the flow through the nozzle. The viscous shear stress produces drag and a small lift and pitching moment. The pitching moment is evaluated with respect to a line through the apex of the cylindrical source flow region. (Equations are also provided for evaluating the moment about an arbitrary point.) The relationship between heat transfer and skin friction, known as Reynolds analogy, is also examined. An efficient and accurate theory and numerical method has been developed for obtaining these boundary-layer quantities, once the pressure gradient parameter β, a stagnation temperature ratio g_w, and a speed parameter S, are prescribed. For this evaluation, we assume the Prandtl number and Chapman-Rubesin parameter are unity, and the gas is thermally and calorically perfect. The boundary-layer flow is considered to remain laminar, because of a relatively low Reynolds number, based on stagnation conditions, compared to that of a typical thrust rocket nozzle and the large favorable pressure gradient due to the very rapid expansion along the nozzle wall.

The results mentioned above are given nondimensionally in terms of M_i, the exit Mach number, the ratio of specific heats, g_w, and two inlet transformed lengths ξ_i. These lengths account for the growth of the separate boundary-layers on the two walls upstream of the inlet surface. Various

discontinuities, as in β, and singularities in some of the integrals are evaluated. Certain parameters, such as g_w, can be specified differently for the two walls. Finally, the formulation and code allows for nozzle truncation.

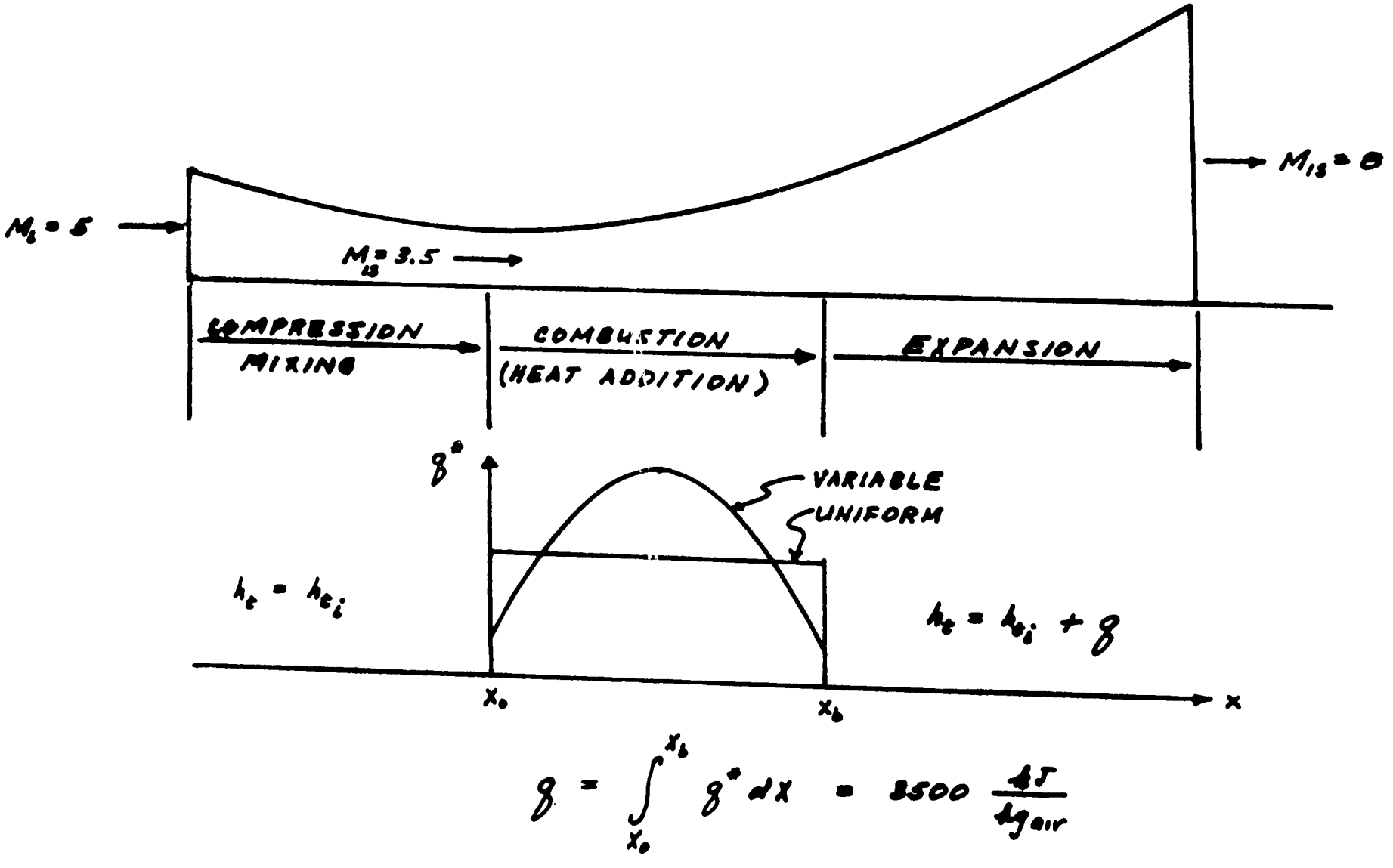

Fig. 1. Nozzle schematic showing different regions.

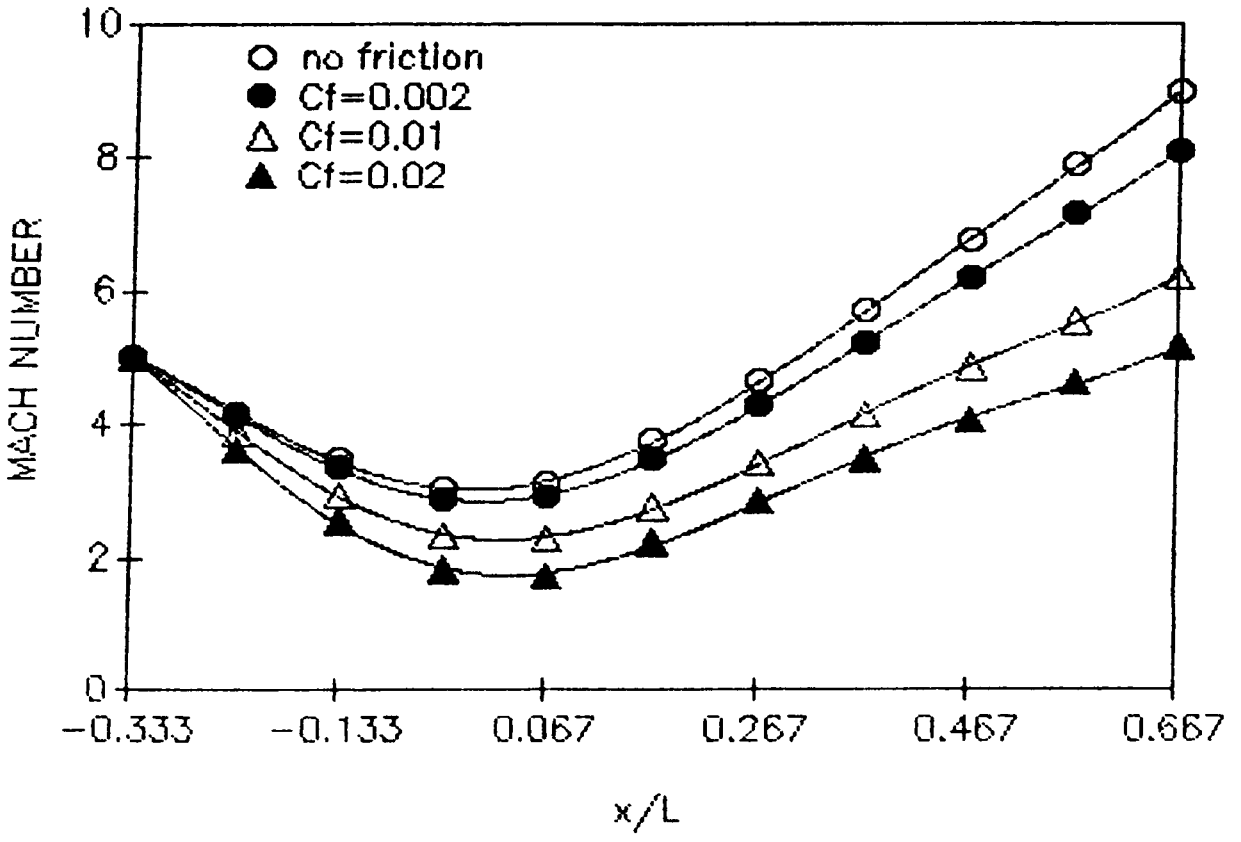

Fig. 2. Mach number distribution as a function of the skin friction coefficient.

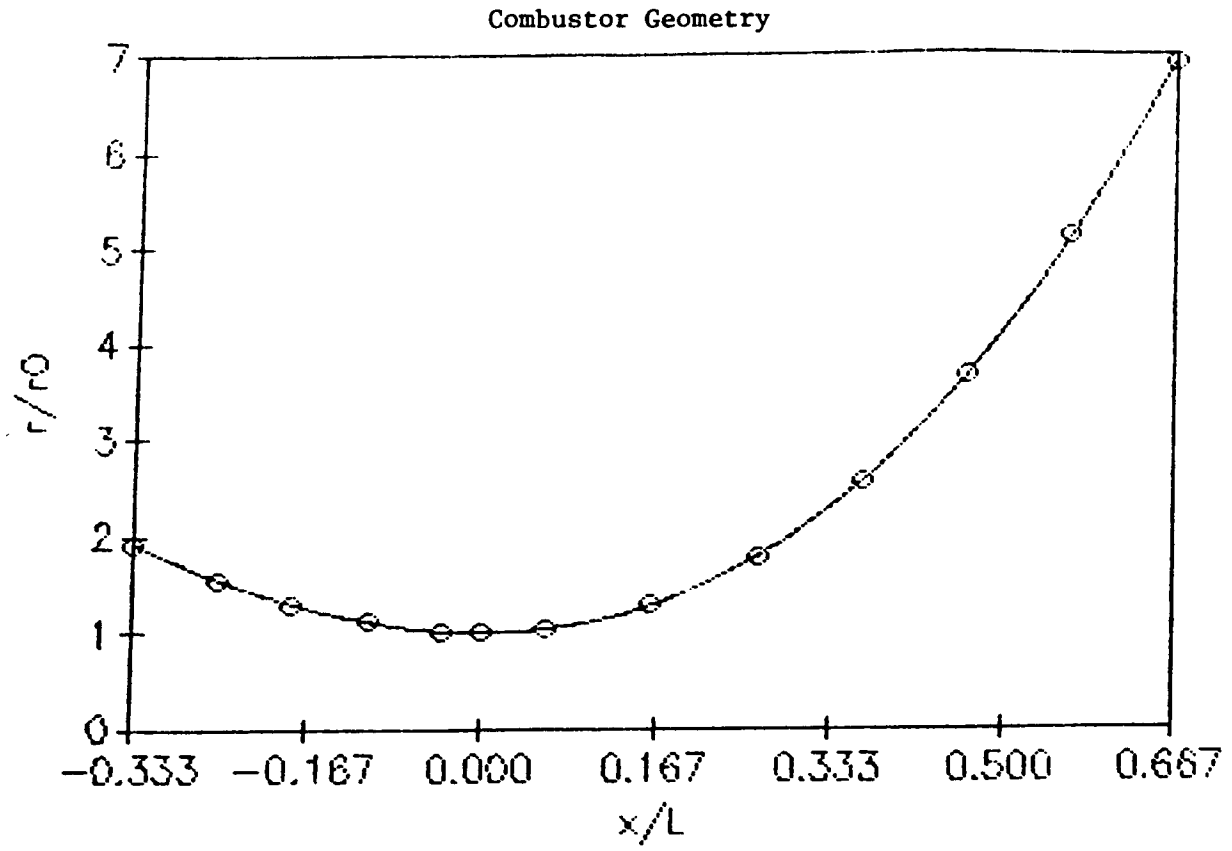

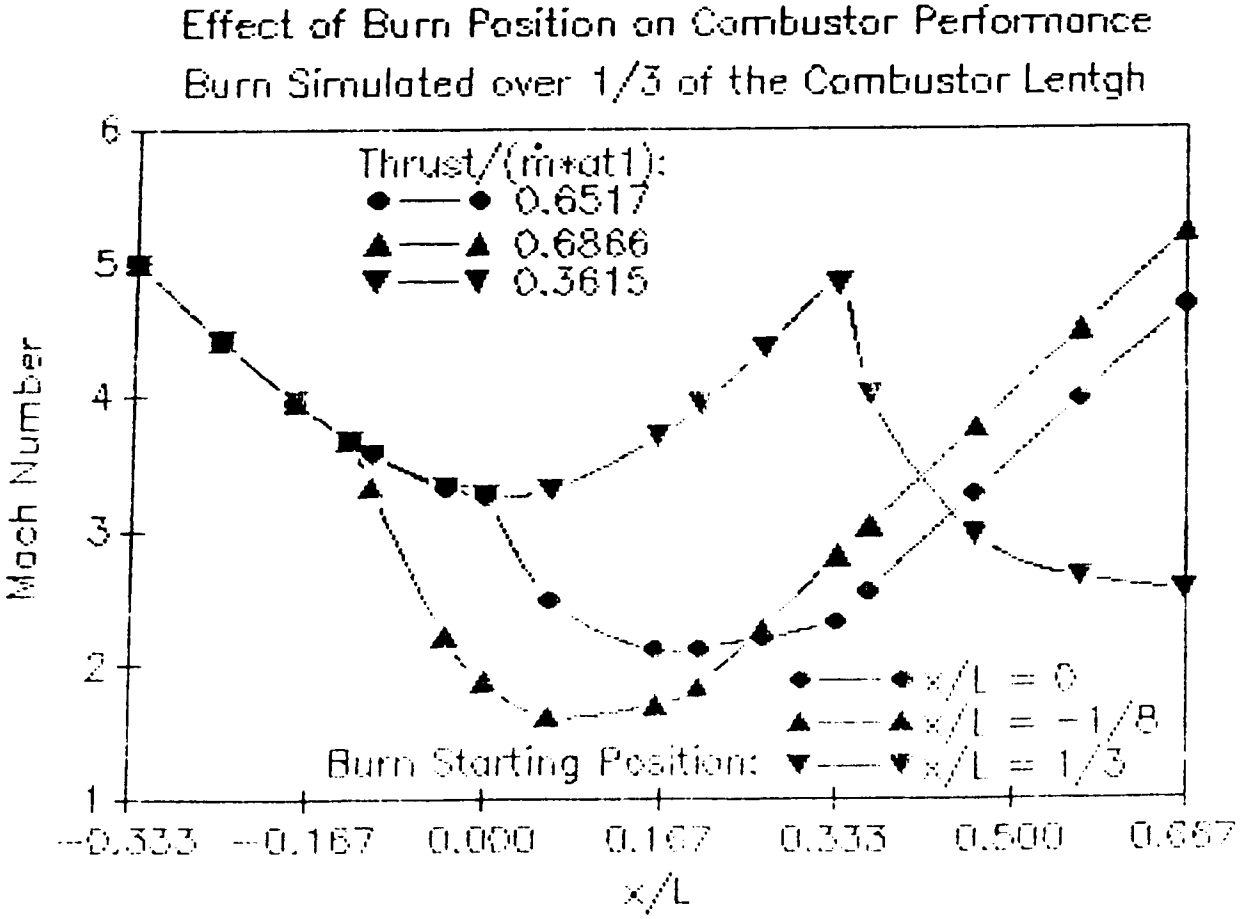

Fig. 3. (a) Radius variation, and (b) Mach number distribution for 3 different burn locations.

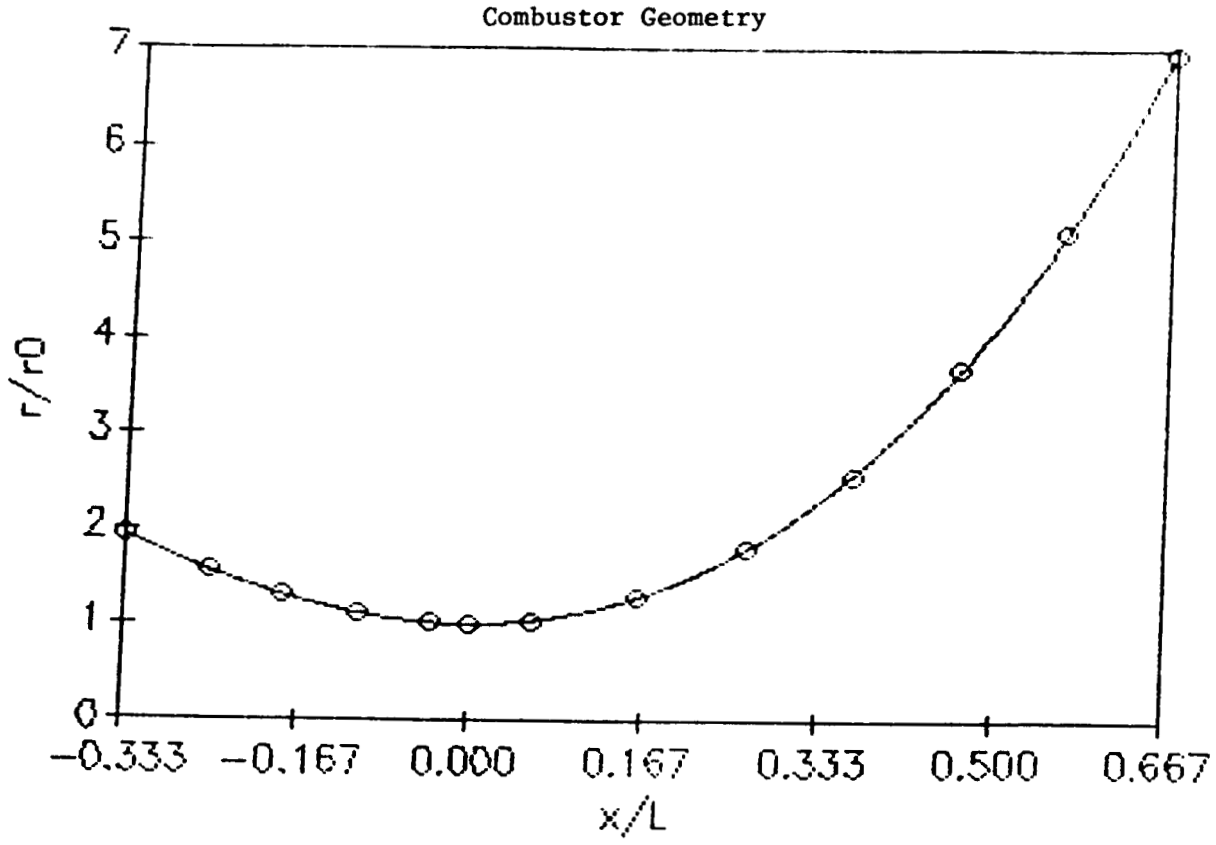

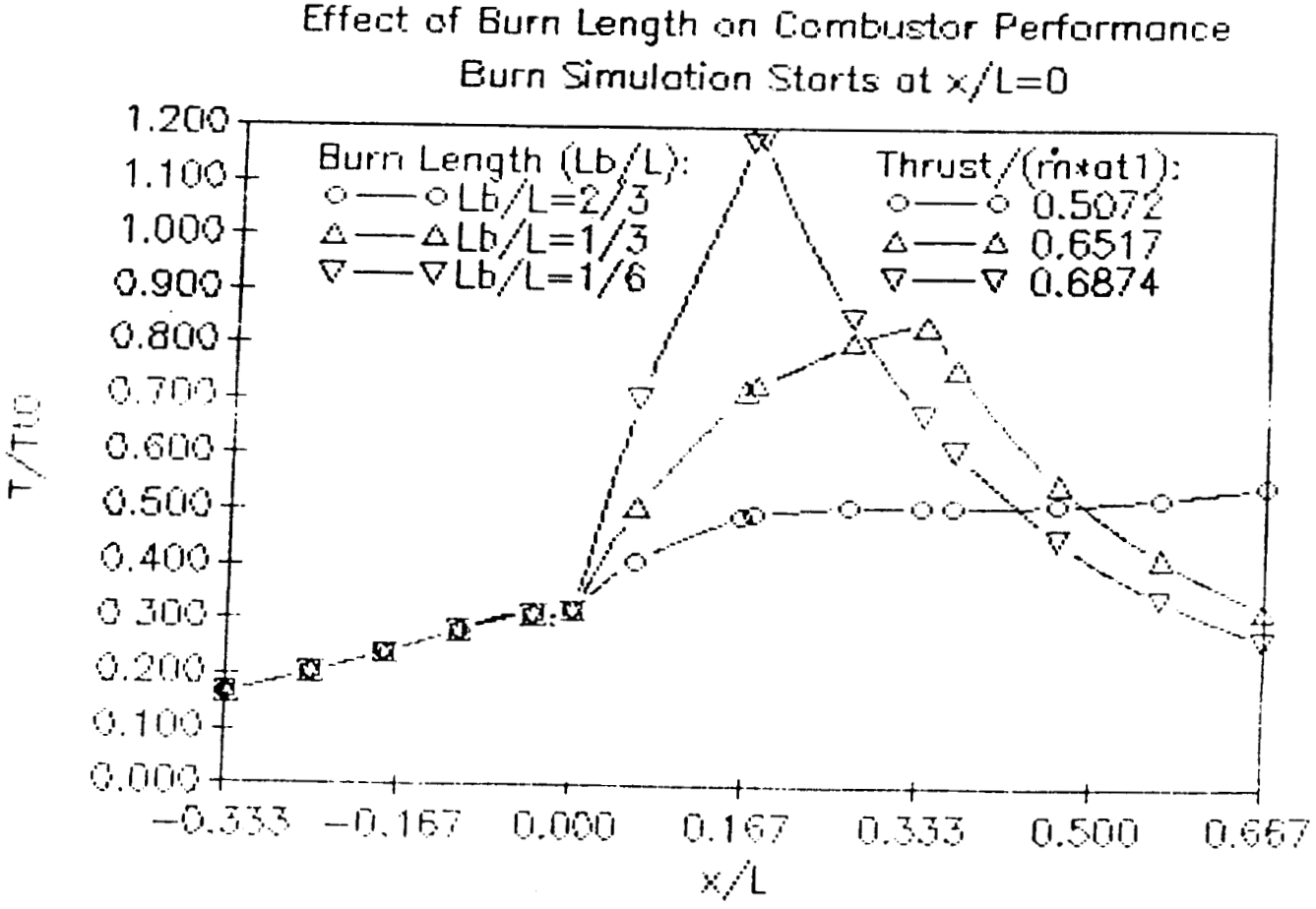

Fig. 4 (a) Radius variation, and (b) temperature distribution for 3 different burn lengths.

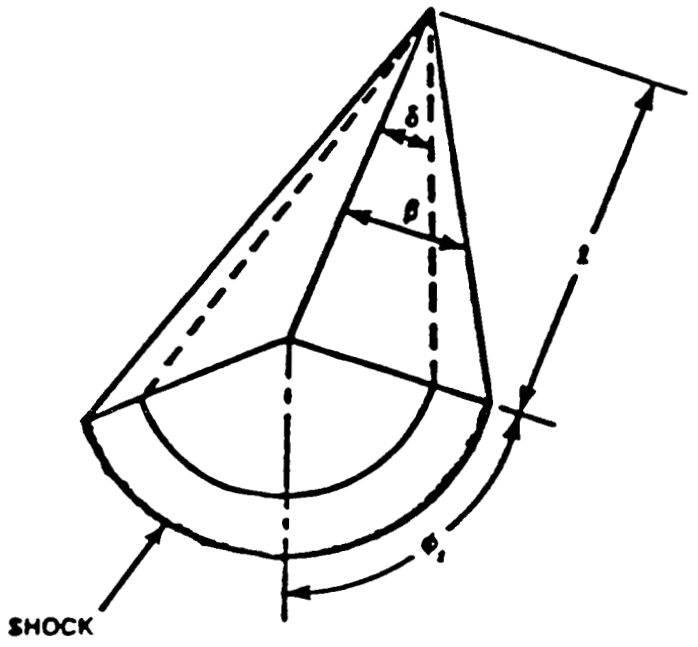

Fig. 5. **The Idealized Cone-Derived Waverider**

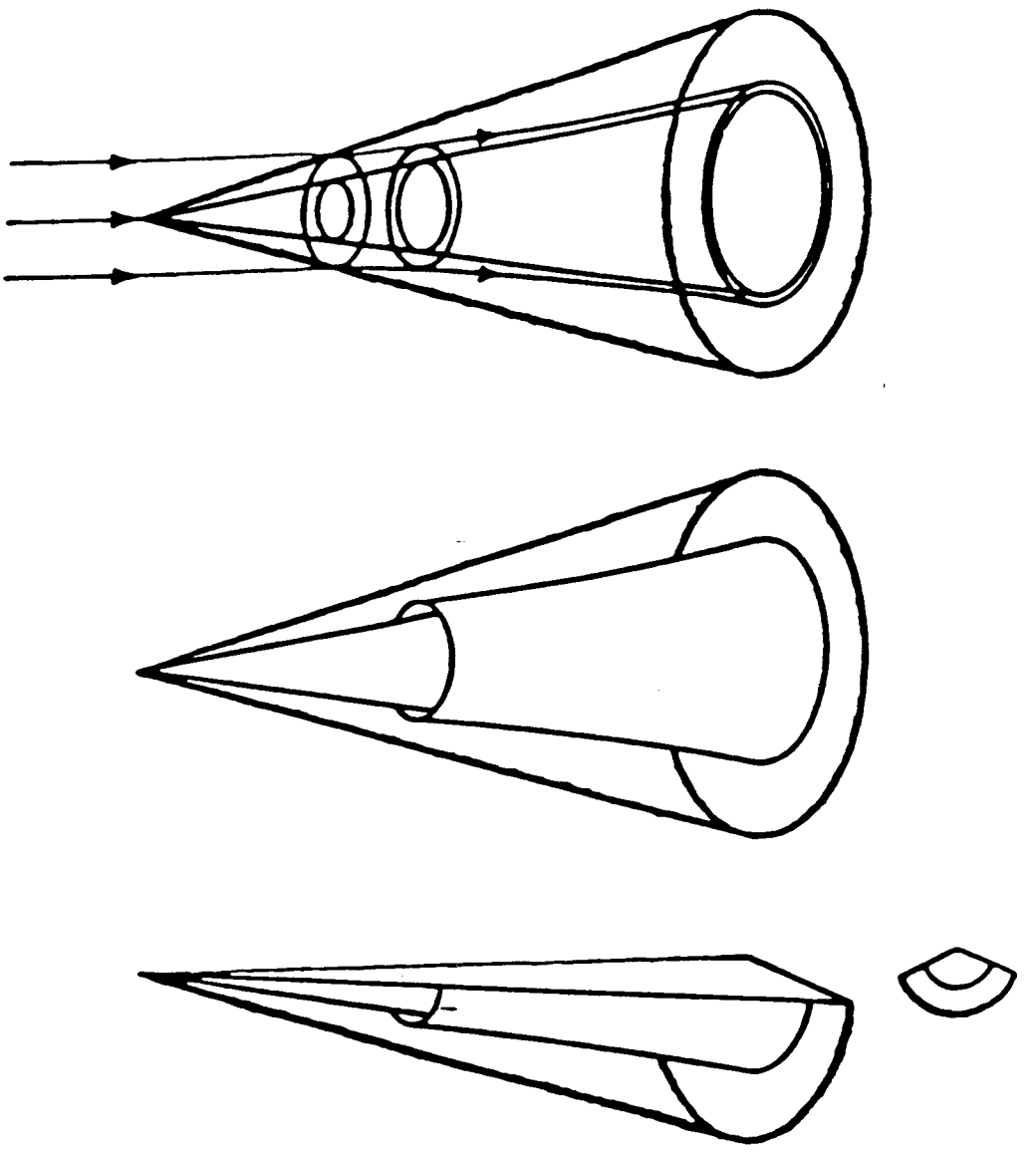

Fig. 6. Construction of axisymmetric inlet on idealized cone-derived waverider.

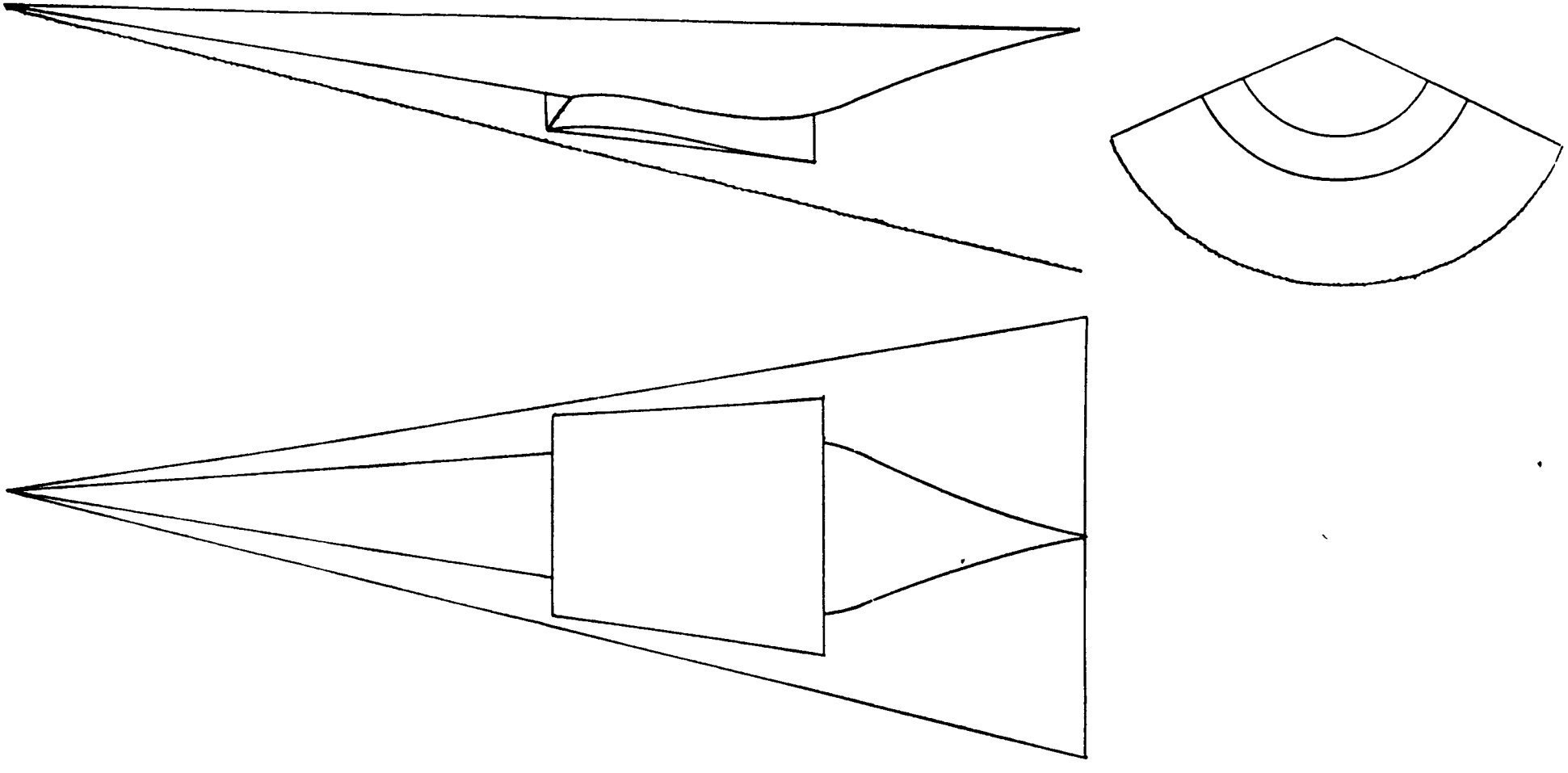

Fig. 7. Idealized Cone-Derived Waverider with Plug-Nozzle Afterbody

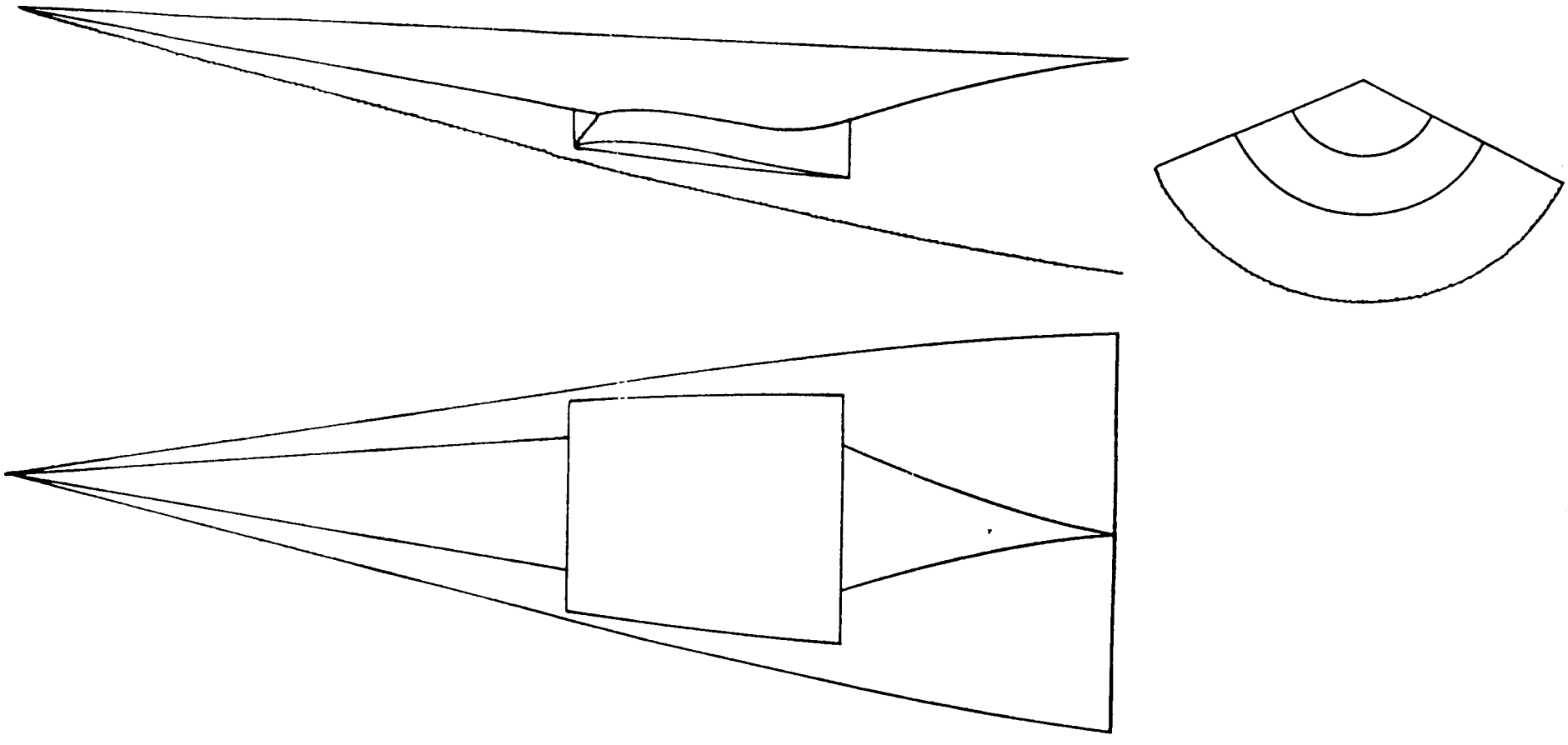

Fig. 8. Idealized Cone-Derived Waverider with Longitudinal Curvature

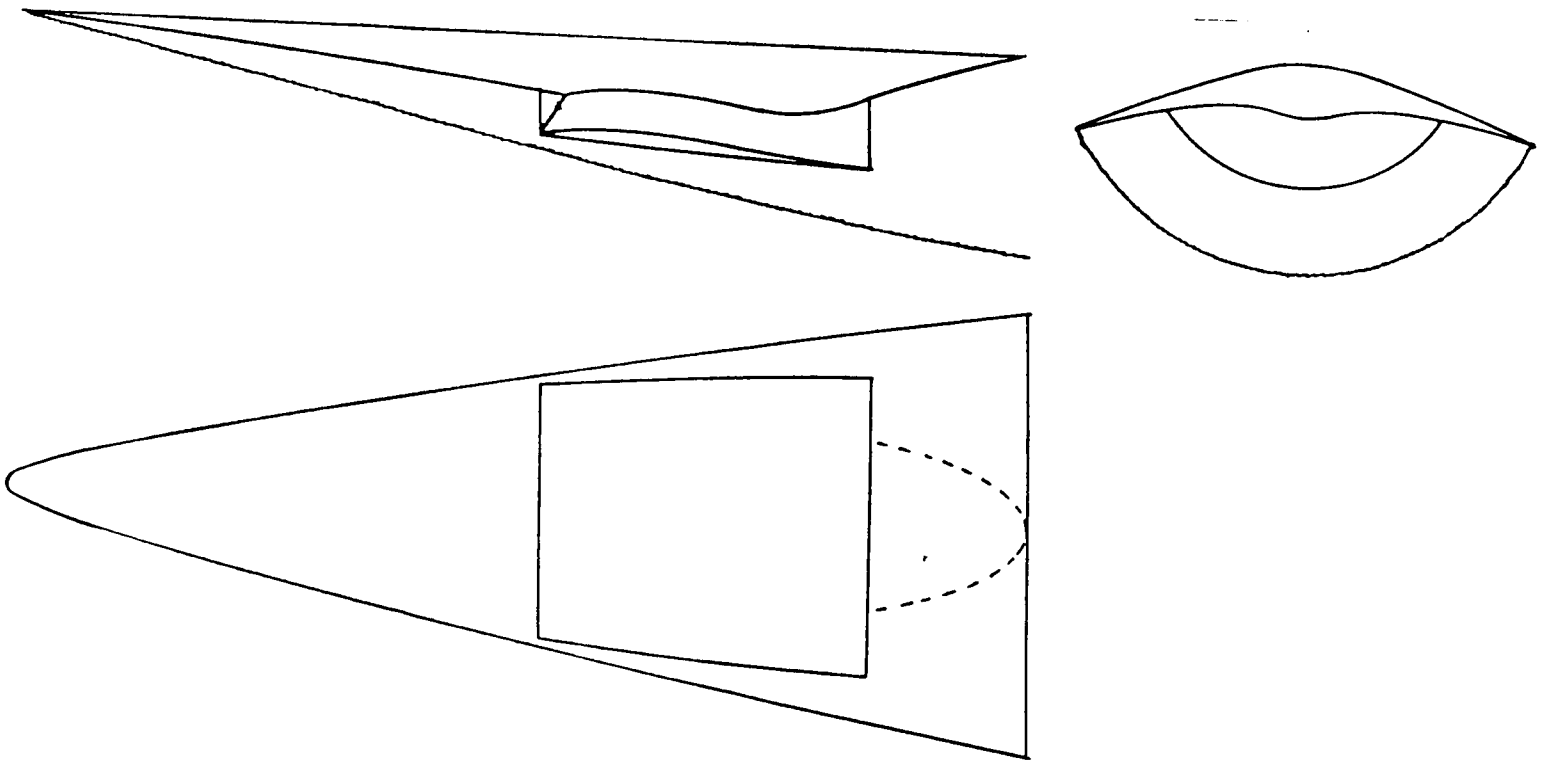

Fig. 9. Blended Cone-Derived Waverider